

# Complete coverage path planning and performance factor analysis for autonomous bulldozer

Rao Li<sup>1,2</sup> | Cheng Zhou<sup>1,2</sup> | Quanli Dou<sup>3</sup> | Bin Hu<sup>4</sup>

<sup>1</sup>National Center of Technology Innovation for Digital Construction, Huazhong University of Science & Technology, Wuhan, Hubei, China

<sup>2</sup>Department of Construction Management, School of Civil and Hydraulic Engineering, Huazhong University of Science & Technology, Wuhan, Hubei, China

<sup>3</sup>Weichai Power Co., Ltd, Weifang, Shandong, China

<sup>4</sup>Shantui Construction Machinery Co.,Ltd, Jining, Shandong, China

## Correspondence

Cheng Zhou, National Center of Technology Innovation for Digital Construction, Huazhong University of Science & Technology, Wuhan, Hubei, China.

Email: [charleszhou@163.com](mailto:charleszhou@163.com)

## Funding information

National Natural Science Foundation of China; Major Science and Technology Project of Hubei

## Abstract

With the development of intelligent machinery, path planning of autonomous bulldozers plays an important role to solve the problems of efficiency in future construction sites. How to plan the path that meets the construction requirements is the key problem. This study investigates the standardized construction workmanship and moving rules of the bulldozer to add rules and path selection strategies to the algorithm. This study establishes the path planning model of bulldozer's leveling, considering the limitations of the traditional bioinspired neural network algorithm, an improved complete coverage path planning method is proposed. An integrated framework is proposed for an automatic bulldozer with a sensor system for a field experiment to verify the feasibility of the method. According to the comparative statistical simulation results, the effectiveness of the method is verified, and the effects of different factors on the path planning results are analyzed.

## KEY WORDS

autonomous bulldozer, BINN hybrid A\* algorithm, complete coverage path planning, earthwork construction, performance factors analysis, sensor system, site layout

## 1 | INTRODUCTION

So far, although it is highly dependent on mechanical operation, the construction industry is still one of the industries with the lowest degree of digitization (Barbosa & Woetzel, 2017). Many studies have mentioned that improving the degree of automation of the construction site can bring many benefits to the construction industry, especially in the site with a large amount of mechanical work and severe high congestion (Kim et al., 2019). At the same time, to improve productivity, solve the problems of lack of work data, and the problems that unskilled workers are prone to make mistakes in the current construction industry, various research are being carried out on the control of construction machines and location estimation (Chen et al., 2018; Lee et al., 2013; Liu & Wu, 2016; Navon & Goldschmidt, 2004; Sturm & Vos, 2008).

Among the construction machine, the bulldozer is a kind of popular machinery, which often appears in many projects and performs various earthwork operations, such as handling, cutting, spreading, leveling, and so on (Hayashi & Shimada, 2013). For example, in the initial stage of site leveling and rough leveling,

bulldozers are needed to cover the whole site completely. However, unskilled bulldozer operators often cause unnecessary construction errors, such as path repetition, and consume a lot of working time and fuel consumption. With the development of intelligent technology, planning a path to improve working efficiency for autonomous bulldozers will play an important role in the future.

Advanced industrial vehicle sensing and control technology, and other auxiliary technologies are proposed (Ali Roshanianfarad et al., 2020) that could support the autonomous bulldozers. To improve the positioning precision and working efficiency of bulldozer, some researchers installed global satellite navigation system, angle sensor, and laser level on bulldozer to measure and control the position of bulldozer (Bonchis & Hillier, 2016; Jonasson et al., 2002). LIDAR and stereo camera are the common environmental perceptual sensors in automatic driving. Generally, the modified bulldozer will be equipped with onboard navigation human-computer interfaces to display the real-time positioning information, such as the location and configuration information of relevant earthwork equipment, and provide guidance to assist construction equipment operators (Leica, 2019;

Trimble, 2019). Although these studies have contributed to the auxiliary operation of bulldozers, there are few research on the application problems of autonomous bulldozers in the construction site.

How to plan a path that meets the work requirements is a key issue. UNSW's team carries out bulldozers' path planning method from the perspective of the dumping operation rules itself, rather than studying the hardware and software technologies such as sensors of unmanned bulldozers (Hirayama & Guivant, 2019; Hirayama et al., 2018). Using the idea of A\* algorithm, they develop a path planning algorithm specifically suitable for bulldozers to let bulldozers complete given tasks with minimal operation time, from the theory development phase (Hirayama & Guivant, 2019). Based on their ideas of studying the operation characteristics of the bulldozer, this paper focuses on the path planning algorithm suitable for the bulldozer's leveling. According to the construction requirements in site leveling, the process required is to completely cover the field to find a path that covers the remaining working space to ensure the maximum coverage and minimum repetition rate (Wang & Bo, 2014). Most of the existing complete coverage path planning (CCPP) research are about airplanes, cleaning robots, and agricultural vehicles (Dakulović et al., 2011; Guastella & Cantelli, 2019; Lakshmanan & Mohan, 2020; Nilsson et al., 2020; Kun, 2020; Sandamurthy & Ramanujam, 2019; Taghavifar & Rakheja, 2021), there are few studies on earth-moving engineering machinery. This article effectively solves the CCPP problem considering the bulldozer's construction rules.

In addition, the conditions of construction sites, such as site entrance, geometry, site boundary, have significant impacts on the results of construction machinery's path planning. These external factors also make the path planning of bulldozers more competitive than ordinary robots in structured environments such as factories or warehouses (Kim et al., 2020). In this study, via MATLAB simulation and analysis, the influences of different factors of the method on the complete coverage path planning of the construction site were obtained, and reasonable suggestions for site layout were put forward.

This study focuses on the CCPP method in a given earthwork site. Different from the traditional method, we consider the working rules of bulldozer, so that the proposed algorithm is more suitable for unmanned bulldozer's site leveling work. The novelty of the proposed method with respect to state of the art is highlighted in the literature review given in Section 2. The CCPP method based on BIMN hybrid A\* algorithm is explained in Section 3. Experiments and results of the proposed method are discussed in Section 4. Evaluation and analysis of various factors are in Section 5. Conclusions are given in Section 6.

## 2 | LITERATURE REVIEW

### 2.1 | Path planning for automatic earthwork machinery

When considering the optimization of the working path in the construction site, the research objects are limited in number. Most are about excavator, heavy machinery and tower cranes on-site

(AlBahnassi & Hammad, 2012; Alshaer et al., 2013; An et al., 2018; Cai et al., 2016; Chang et al., 2012; Fang & Cho, 2018; Han et al., 2016; Hung & Liu, 2016; Kim & Lee, 2020; Lin et al., 2014; Lin & Wu, 2014; Sivakumar et al., 2013), but these construction rules were different from the bulldozer, which could not be applied directly. Only the Hirayama's team carried out bulldozers' path planning from the perspective of construction and combined with the dumping rules of the mining dumping area, and verified the effectiveness of the algorithm (Hirayama & Guivant, 2019; Hirayama et al., 2018).

And with the development of automation technology, the automatic path planning of bulldozers in the construction site has been studied, which is generally based on robot obstacle avoidance technology. Sun and Kim (2017) introduced a method of attitude and position estimation of bulldozer blade by combining inertial measurement unit (IMU) with two Real-time kinematic (RTKs). Based on the sensor fusion of inertial measurement unit combined with two RTK receivers, a guidance system for bulldozer was developed, which provides an accurate estimation of the position and attitude of the bulldozer and feeds back to the navigation system. And the experimental results testified the effectiveness of the method via installing the sensor systems on bulldozers for experiments. Minamoto and Kawashima (2016) upgraded a remote-controlled bulldozer, which transmits data to the control system through sensors installed on the blade to realize force feedback. To provide visual feedback, cameras are installed on the operation box and roof of the remote bulldozer robot.

Therefore, this paper designs a bulldozer transformation monitoring system with independent path planning ability, and equips the bulldozer with an intelligent construction computing platform to realize real-time position perception, and task release, which verified the applicability of the on-site operation rules-based CCPP method for bulldozer.

### 2.2 | CCPP algorithm for bulldozers

In the construction site, global static environment path planning was the most basic issue for the bulldozer rough leveling, because in this construction process, the task of bulldozer was to complete coverage of the whole site ground. Therefore, some algorithms were suitable for planning the whole-site-coverage paths, which we called CCPP algorithms below.

One of the approaches for the CCPP is cellular decomposition (Karapetyan & Benson, 2017). The use of genetic algorithm and ant colony optimization could also be used (Dogru & Marques, 2015; Liu & Yang, 2017). Genetic algorithms that encounter numerous complex irregular obstacles in the environment cannot be solved effectively; their search efficiency and speed are low. Meanwhile, these models can only deal with situations in a static environment and precise prior knowledge of the workspace is a must. Though the neural network models can generate an obstacle avoidance trajectory dynamically, due to long learning time and large delay, it is difficult to ensure the

real-time planning of the operation path of unmanned bulldozer on site.

The method of path planning based on a bioinspired neural network (BINN) proposed by Meng and Yang (1998) and Luo (2004) has been used to generate a real-time obstacle avoidance path in dynamic environments. Compared with other models, it is not affected by the shape and location of obstacles in the environment, does not require a learning process, and need no deliberate search for free space and a collision path, which does not need precise knowledge of the environment. A CCPP method for an underwater vehicle based on BINN that defines the neural dynamics using differential equations has been proposed to overcome the limitation of offline path planning methods (Zhu & Xiang, 2018). The applicability of the CCPP method based on BINN has also been demonstrated in Luo and Yang (2016). Muthugala and Samarakoon (2022) proposed a novel coverage method based on Glasius BINN for a multipurpose ship hull maintenance robot which performance significantly surpasses that of the state-of-the-art methods in terms of energy usage.

Due to the high experimental cost of unmanned bulldozer and the need to lay the foundation for real-time path planning in the future, the feature of BINN algorithm without learning process is just in line with the goal of improving efficiency and no need for precise prior knowledge of the environment which can also reduce the technology pressure and cost of the sensors to guarantee the safe obstacle avoidance. BINN has the defects of a large amount of calculation, waiting for a long time to escape when falling into a "dead zone." Therefore, on the basis of adding the corresponding bulldozer walking rules to the algorithm, it is necessary to further improve the performance of getting rid of the "dead zone." This paper chooses to improve this algorithm to provide path planning strategy for bulldozer construction.

### 2.3 | Performance analysis of path planning algorithm

Several evaluation indexes can be used for an algorithm. For example, Ni et al. (2017) utilized path length, time, and efficiency to evaluate the BINN algorithm. Zhu and Tian (2019) evaluated two algorithms by adopting coverage rate, time complexity, repetition rate in the region, total voyage steps of autonomous unmanned vehicle (AUV), and the number of AUV course changes to verify if the algorithms are suitable for complete AUV coverage. Kim et al. (2020) reported that for large-scale engineering work, path planning update is often performed once a week or once a day. Thus, he did not consider the factor of comparison time in his algorithm review. The current study uses coverage rate, repetition rate, total path length, and turning times as evaluation indexes.

Influencing factors can be divided into external and internal factors. Kim and Russell (2013) reported that initial conditions, such as the entrance to a construction site, and geometry and boundary of the construction site, greatly affect the result of the task plan.

Specifically, entrance to the worksite was a vital factor, especially for the site of which the accessibility is severely restricted, it determined the starting position of the work. These factors were all called external factors that make path planning for construction machines more challenging than planning for ordinary robots in structured environments, such as factories or warehouses. Thus, concerning the choice of external factors, we select the entrance of the site, the location of obstacles, and the shape of obstacles as the main factors for analysis.

With regard to internal factors, each algorithm has its internal parameters and iterative process. For example, the neural network algorithm is more concerned with the influence of learning process, but because BINN does not involve the learning process, it is slightly difficult to analyze the internal factors of the algorithm. Owing to the use of MATLAB programming, to solve the excitation equation cell activity value via the ode45 solution; this could lead to different results.

### 2.4 | Complete coverage path planning (CCPP) method

The main approach adopted in this study is that on the basis of the initial navigation map, the bulldozer's position calculated by RTK and data of the environment collected by the sensor, which includes the position of obstacles and start node, as well as departure direction are taken as the input of the CCPP method. The proposed path is planned by the BINN hybrid A\* algorithm combined with the bulldozer's walking rules. The whole process is as below in Figure 1. The simulation was performed in MATLAB, and the coverage path was planned by our modified algorithm. And owing to the simulation experiments, we could analyze different factors in conditions and their influence. The method was validated and implemented on a bulldozer.

## 3 | RULES OF BULLDOZERS ADDED TO THE ALGORITHM

Many studies showed that the local navigation strategy depends largely on the process of cell decomposition, and the rest of the path planning is based on the before and after modes until the site boundary is reached (Kim & Russell, 2013; Kim & Seo, 2012). Although these studies put forward a path planning strategy for automatic earthwork planning, the unique characteristics of autonomous bulldozers were not fully considered. A bulldozer's path is slightly different from the general complete coverage path. When a bulldozer walks and covers the working environment at will, it moves back at a certain angle when it meets the boundary and obstacles of the working environment as shown in Figure 2, the working path of the bulldozer is composed of forward and backward, and it rarely turns and turns around. The length of the bulldozer operation area is determined by the best effective path of the bulldozer. Given the

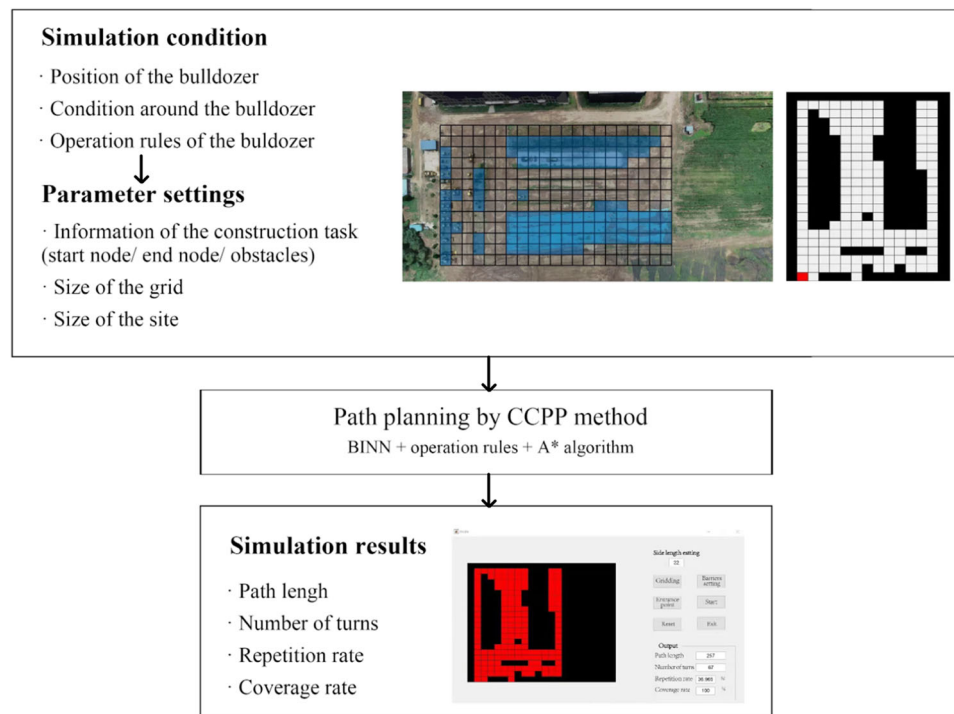


**FIGURE 1** The flow chart of the simulation process of complete coverage path planning system.



**FIGURE 2** Operation rules of bulldozers.

presence of a standard for the best effective haul distance, studying the complete coverage and reducing the turnaround rate and repetition rates are meaningful.

The path walking rules are set to be in line with the bulldozer walking rules as follows: straight walking while avoiding obstacles in front, on the left, and the right. The rules for detouring to avoid obstacles are shown in Figure 3, where 2 refers to obstacles, 1 refers to covered grid points, 0 refers to the points to be covered, and X refers to the state of the point when the robot executes the movement rules. The two numbers 1s in the blank grid and the black arrow indicate the robot's previous position, current position, and previous moving direction. The black grid (1/2) indicates that during the robot's moving process, unrelated covered points and obstacles are regarded as the same type of obstacles. The red arrow and the number 0 indicate the next moving direction and position selected by the robot after triggering the moving rule method.

### 3.1 | BINN hybrid A\* algorithm

CCPP algorithms are suitable for bulldozers because bulldozers need to spread soil piles or remove ground obstacles in their working environment to make an area flat. BINN algorithm was usually proposed for complete coverage path planning of robots in complex environments (Luo & Yang, 2002). In this study, the BINN algorithm was used to generate the moving path that covers the entire working space and avoids obstacles, thus providing a choice for bulldozer automatic construction.

The basic principle of the algorithm is: the robot workspace is gridded using the grid map method, and each grid point has different sizes of neuron activity values. Moreover, each grid point only has a connection with its adjacent grid points, thus forming a sudoku grid like a local grid point connection neural network. The change in the neuron activity value of each grid point can be expressed as follows:

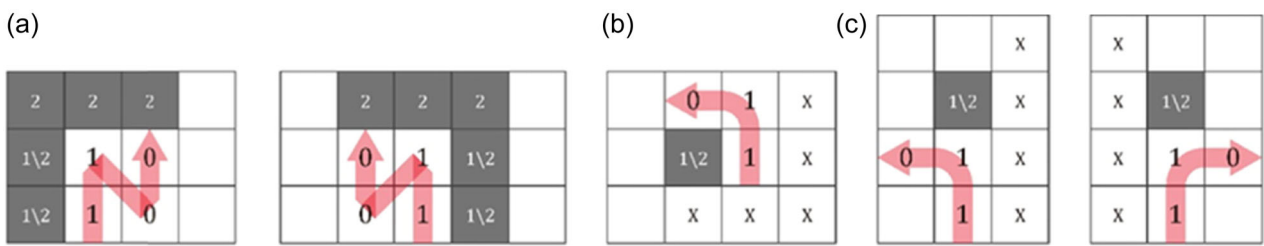


**FIGURE 3** Added rules. (a) The bulldozer moves forward in a certain direction and retreats in the syncline to complete the bulldozing once. (b) and (c) The walking rules are set to ensure that obstacles will be bypassed.

$$\frac{dx_i}{dt} = -Ax_i + (B - x_i) \left( [l_i]^+ \sum_{j=1}^k W_{ij} [x_j]^+ \right) - (D + x_i) [l_i]^-,$$

$$y_j = 1 - \frac{\Delta\theta_j}{\pi},$$

This equation is called the shunt equation. Parameters  $A$ ,  $B$ , and  $D$  are all nonnegative constants. In the equation,  $A$  represents the decay rate,  $B$  represents the upper limit value of the grid point neuron active state,  $D$  represents the lower limit absolute value of the grid point neuron active state (the opposite number of the lower limit value)  $x_i$  represents the neuron active value of the current grid point  $i$ , and  $k$  represents the number of grid points adjacent to the  $i$ th grid point. The maximum value of  $k$  is 8.  $l_i$  is the external input (input of self-status) of the neuron activity value at the  $i$ th grid point, and it is defined as follows: if  $i$  grid point is the point to be covered, then  $l_i = E$ ; if  $i$  grid point is an obstacle, then  $l_i = -E$ . In other cases,  $l_i = 0$ .  $E$  is much greater than  $B$ ,  $[l_i]^+ \sum_{j=1}^k W_{ij} [x_j]^+$  means the excitation input,  $[l_i]^-$  means the suppression input,  $[l_i]^- = \max\{-l_i, 0\}$ ,  $[l_i]^+ = \max\{l_i, 0\}$ .  $W_{ij} = f(d_{ij})$ , where  $W_{ij}$  denotes the influence weight of grid point  $j$  connected to the local side of current grid point  $i$ .  $d_{ij}$  represents the Euclidean distance between the location of the  $i$ th grid point and the location of the  $j$ th grid point. In general, we need to specify that the grid points are connected only in a small area  $(0, R_0)$ . If  $d \geq R_0$ ,  $W_{ij} = f(d_{ij}) = 0$ . If  $0 < d < R_0$ ,  $W_{ij} = f(d_{ij}) = \frac{u}{d}$ , where  $u$  is a nonnegative constant. Generally,  $R_0 = 2$  to ensure that the grid points are connected with eight surrounding points at most. In accordance with the shunt equation, the motion path of the robot can be obtained as follows:

$$p_n \leftarrow x_{p_n} = \max\{x_j, j = 1, 2, \dots, k\},$$

where  $k$  is the number of other grid points adjacent to the current grid point and  $p_n$  is the next position (grid point) toward which the robot moves. When it is used in complete coverage path planning, parameter  $c y_j$  needs to be introduced to select the next location. The formula is as follows:

$$p_n \leftarrow x_{p_n} = \max\{x_j + c y_j, j = 1, 2, \dots, k\},$$

where  $c$  is a normal number whose value has an impact on the turning direction of the robot,  $k$  is the number of other grid points adjacent to the current grid point,  $p_n$  is the next position of the robot, and  $y_j$  is a function of the turning angle of the robot. The previous position of the robot is  $p_p$ , the current position is  $p_c$ , and the next possible position is  $p_j$ . The steering function is defined as follows:

where the angle between the moving direction of the bulldozer from the previous position to the current position and the moving direction from the current position to the next possible position is expressed as follows:

$$\Delta\theta_j = |\theta_j - \theta_c| = \left| \arctan\left(\frac{y_{pj} - y_{pc}}{x_{pj} - x_{pc}}\right) - \arctan\left(\frac{y_{pc} - y_{pv}}{x_{pc} - x_{pv}}\right) \right|,$$

The activity value of each grid obtained by modeling the task area is shown in Figure 4. Figure 4a shows the initial activity value of each neuron when the agent is about to enter the task area. In the figure, the depression ( $-E$ ) is the area with low activity value, which corresponds to the location of the obstacle, and the activity value of the area to be covered is  $E$ . The agent will only travel along the gradient of neuronal activity and cover this area along the level of neural activities. Figure 4b shows the activity of each neuron in the planning process. It can be seen that the activity value of the traversed region becomes 0. When the coverage of the whole task area is completed, it means that the coverage planning task is completed. Except for the area where the obstacle is located, the activity value of each neuron becomes 0, as shown in Figure 4c.

This method easily falls into a dead zone when encountering a blocking point, and the planned escape route is not optimal. For the dead zone problem in point-to-point path planning, the A\* search algorithm has been used (Liu et al., 2019). The main ideas of the escaping dead zone in this paper are as follows: (1) Take the current point as the center, spread outward according to the size of a grid, and record the diffusion points. If all four directions in the diffusion have exceeded the boundary, the coverage is completed; (2) Detect the attribute of each diffusion point and judge whether there are uncovered neurons in the current diffusion point. If not, continue to execute (1), otherwise, save the uncovered neurons in this step separately; (3) Traverse all diffusion points, set a diffusion point as a possible target point, and use A\* algorithm to plan the path from the current point to the possible target point; (4) Find the nearest uncovered point in turn as the initial target point, and then use the A\* algorithm to obtain the path point. Take the first uncovered point in the path point as the next target point and escape from the dead zone to continue to complete the subsequent coverage task. The A\*

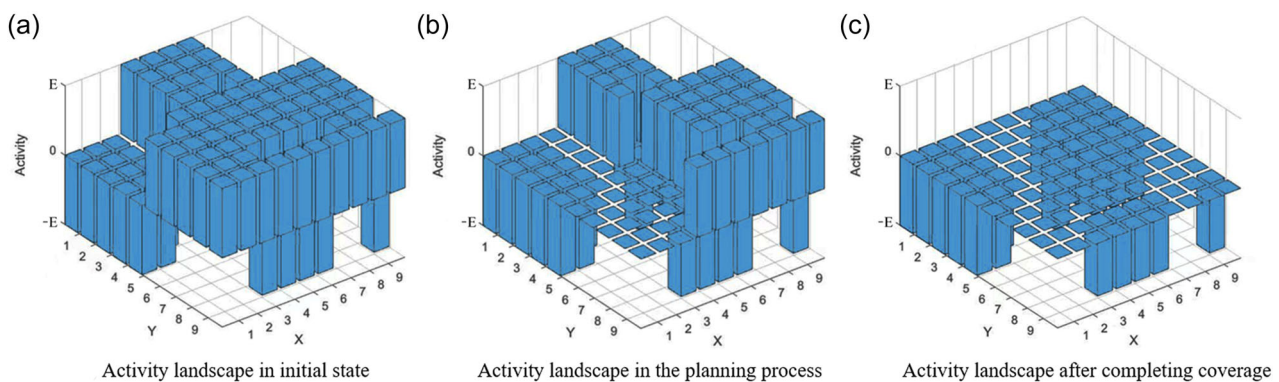


**FIGURE 4** Activity landscape in different stages.

algorithm is a typical heuristic search algorithm. The cost function of the A\* algorithm is

$$f(n) = g(n) + h(n),$$

where  $g(n)$  represents the path length from the starting point to the current point  $n$ ,  $h(n)$  represents the estimated path length from the current point  $n$  to the target point, and  $f(n)$  represents the total path length required for the starting point to reach the target point from the current point  $n$  after passing through the current point  $n$ . The A\* algorithm always preferentially selects the current opening in the process of searching the path. The point with the lowest value of  $f(n)$  in the list is taken as the current point, and it expands to the target point continuously. Then, an optimal path is obtained.

Combined with the A\* search algorithm and moving rules, a typical earthwork construction site can be divided into bulldozing construction area, restricted access area (including obstacles), access

and exit area, and starting unit of bulldozing. With the user's input, the starting unit and conditions for the accessibility of the bulldozer can be set; subsequently, all units perform an accessibility review. The accessibility review of each unit produces eight directions of analysis. The overall process of the CCPP method is given in Algorithm 1. Initially, the metric map of the environment is fed to the bulldozer. The corresponding grid map is then created, and the neural network is constructed to represent the states of the grid cells. The robot's initial position is considered as the current location, and the robot initiates the coverage. The next cell for the navigation is determined by the criterion given in Sections 3.1 and 3.2 based on the neural activity and operation rules. The next cell becomes the current cell after the robot moved onto it, and the current cell is tagged with the state, already covered. The neural activity is dynamically updated with the actions of the robot. This process is repeated until the bulldozer covers the entire workspace.

---

#### Algorithm 1: Overall Operation

```

Input : Grid map, Updates for map
Output: Bulldozer navigation path
Initialization;
Create grid map;
Construct corresponding neural network;
Set parameters and initial position and direction of the bulldozer as current position;
Initiate coverage;
while number of uncovered cells !=0 do
  if bulldozer operation rules are triggered then
    | Change the status of current cell to covered based on the operation rules;
  end
  if bulldozer is in dead zone then
    | Search for nearest with activity value and select the shortest path by A* algorithm;
  end
  Change the status of current cell to covered;
  Update neural activities;
  Select next cell for navigation;
  Bulldozer moves to next cell;
  Set new location as the current location;
  if update for grid map is available then
    | Update grid map;
  end
end
```

---

### 3.2 | Algorithm evaluation and factors analysis

The biological excitation neural network has been successfully applied in path planning, complete path coverage, and trajectory tracking. However, the local side connection point of the robot's current point (the two points have the same neuron activity value) appears easily in this method. This situation increases the length of the planned path, repetition rate, and the number of turns; in addition, when a blocking point is encountered, the robot easily falls into the dead zone, and the planned escape route is not optimal (Zhu & Tian, 2019).

Therefore, in the subsequent evaluation of the influencing factors of the algorithm, we select four indicators: path length, turn times, path repetition rate, and coverage rate. These indicators were also used by Zhu and Tian (2019) in their research. The path length, turning times, and repetition rate cannot only evaluate the algorithm but also evaluate the benefits of bulldozer construction under certain site conditions. The shorter the path is, the less the number of turns is, and the less the path repetition rate is, which is more beneficial to reduce the construction cost and increase the construction efficiency. Of course, since it is a complete coverage path planning algorithm, site coverage is also essential. If the operation of the algorithm was over, there were still points in the site that have not been passed, it proves that the algorithm has defects, and in the actual construction, it cannot meet the requirements of the whole site spreading or leveling.

In Section 3.2, we established the existence of a construction range with the best effective transportation distance in actual sites, which is generally a standard. Thus, to improve site construction efficiency, we need to consider reducing the path length of full coverage and the turning and repetition rates. The path length is the total number of squares covered by bulldozers, and the number of turns is the number of squares covered by bulldozers (the turning angle is 90° when the bulldozer is backward). The path repetition rate is the number of cells repeatedly walked divided by the number of squares already walked.

$$\text{Path repetition} = \frac{\text{Repeated passed cells}}{\text{Already passed cells}},$$

Coverage rate is the area covered by the program after the completion of operation in the site divided by the area without obstacles in the site. In the design program, these indicators are updated live.

$$\text{Coverage rate} = \frac{\text{The whole covered cells}}{\text{Site area}},$$

## 4 | EXPERIMENTS AND RESULTS

### 4.1 | Sensor system of autonomous bulldozer

The test platform of path planning selected the Shantui SD17 bulldozer, which was modified according to the technical

requirements of the automatic system, as shown in Figure 5. The RTK receivers were connected to the bulldozer. Two antennas were attached to the blade itself using the level receptor masts. The position of the receivers was calculated by using Unistrong firmware and postprocessing software as well as internal software developed by Shantui company, which combined into a complete blade leveling system and have a control platform. At the same time, there are six cameras on the top of the bulldozer cockpit, which are located in different directions to record the environment around the bulldozer and millimeter-wave radar and ultrasonic radar perceive and collect environmental data. Combined with the position estimation of the bulldozer and sensor preprocessing, they are uploaded to the high-performance computing platform equipped in the vehicle, which is connected with the final digital construction system platform to establish the scene and carry out collision-free path planning.

This paper introduces the structure of the automatic navigation system and the overall framework of data acquisition and transmission is shown in Figure 6. The whole system includes positioning unit, path planning unit, and control unit. During the operation, the positioning unit collects site information for path planning, and the Tbox equipment obtains the sensor data and blade leveling system data for analysis, processing and transmission of decision commands. In addition, the control unit carries out the command issued by the digital construction platform and feeds back the results. The machine is wireless communication, and the information transmitted is mainly the status signal of the host or slave.

In this part, we built a grid map for path planning from sensor data and UAV image model. First, UAV acquired the initial three-dimensional (3D) map and initial geometry information of the clutter field. Unlike two-dimensional (2D) or 3D design information, 3D geometric model includes not only the target structure, but also the vegetation, temporary things and obstacles that cannot be found in the design model. The initial 3D map is vital for an autonomous bulldozer to carry out complete coverage path planning, and it does not need time-consuming and laborious attempts. And according to the UAV-image-based model, a global navigation map is generated. At the same time, the blade pose should be corrected relative to the horizontal coordinate. Then, the point cloud is generated with sensor information, and the ground points are segmented from the point cloud based on Octree (Wang & Wang, 2018). Octree can be regarded as a 3D grid map, and make it convenient to refer to the grid coordinates of specific parts. In addition, it is convenient to accurately map and modify the site information in the map used in path planning.

On the basis of the point cloud generated by UAV and sensor system, and the construction rules of bulldozers, the navigation map is gridded, and the CCPP algorithm is used for path planning. The planning algorithm includes the walking rules when the bulldozer performs tasks, and the A\* algorithm is adjusted and optimized. And the generated path will be transmitted back to the Tbox on the vehicle through the digital construction platform, so as to command the bulldozer to move.

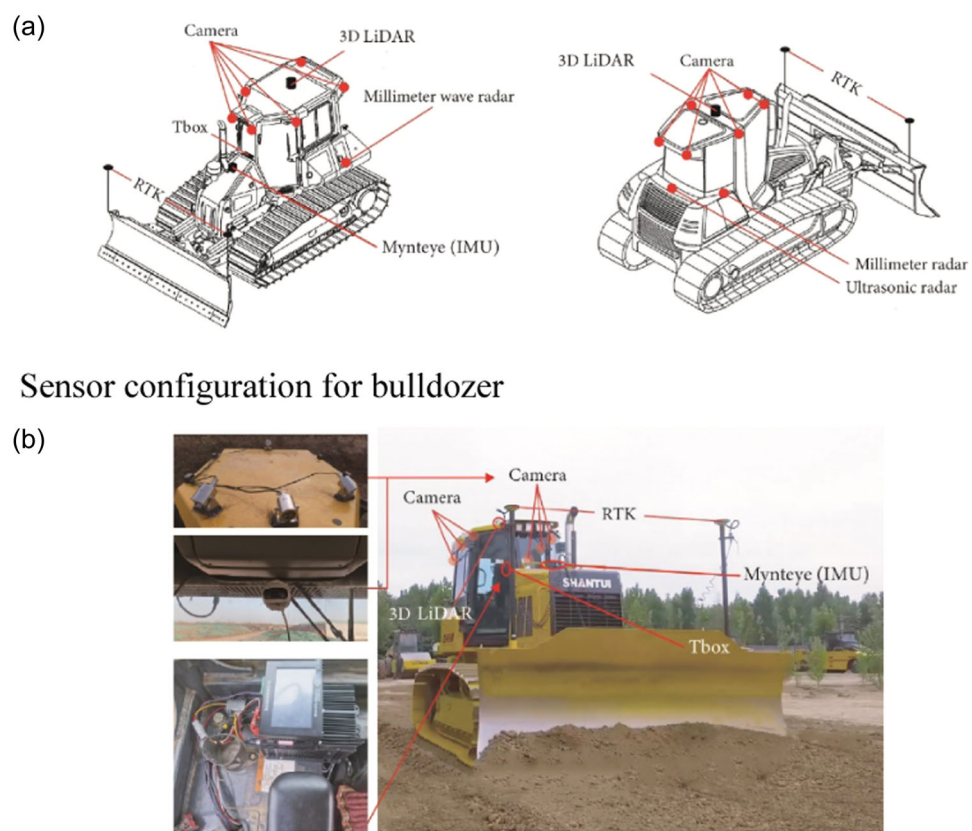


**FIGURE 5** Modified bulldozer with the automatic system. (a) Sensor configuration for bulldozer and (b) experimental setup: Dozer, sensors and location.

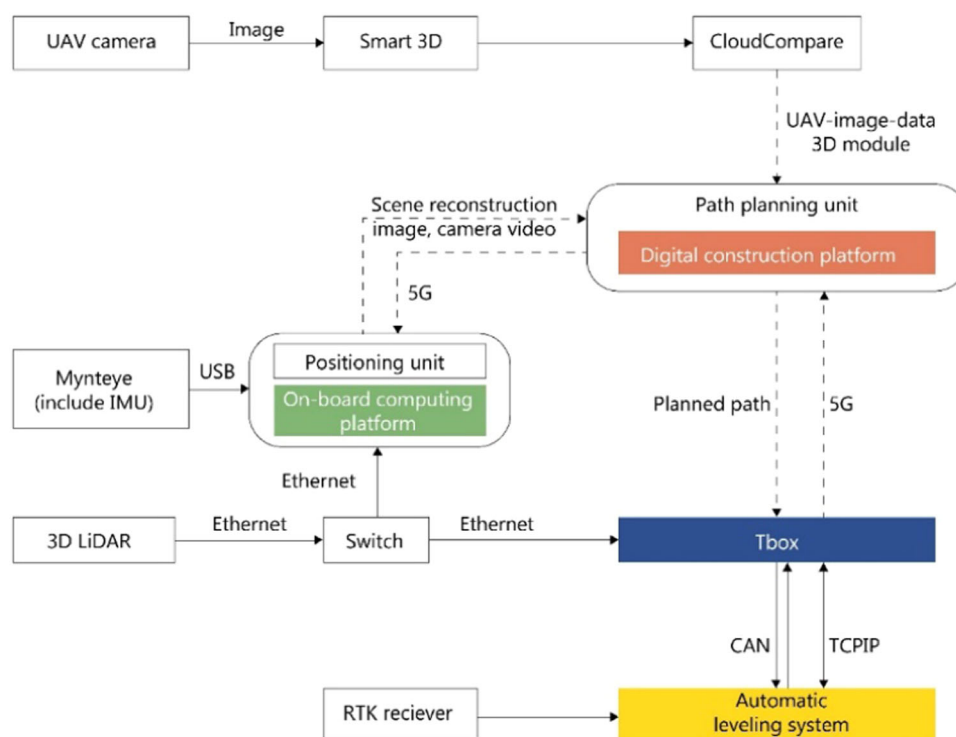


**FIGURE 6** General frame of the data acquisition and transmission.

## 4.2 | Field test and data collection

Our project is Jining Avenue West extension project, in Shandong Province, China. The experiment we need to do is the preliminary preparation work of a construction site—rough leveling, using bulldozers to level the site. Therefore, we used the sensors and UAV to generate a navigation map, and applied the CCPP method to plan the path of automatic bulldozer. The scene panorama of UAV scanning 3D modeling is shown in Figure 7. Some parts of the test site lay machinery and inaccessible area and sections, which could be seen as obstacles and made the site situation complicated, so there was a certain difficulty in CCPP.

To ensure the progress of the experiment, we calibrated in the selected range, set up a small pile every 20m to ensure a clear boundary, and used RTK at the four corner points to ensure accuracy. Before the start of the experiment, irrelevant personnel was not allowed to get close to the test site and the working conditions of the sensors were checked. Due to complicated working conditions such

as rain, snow, wind, and so on, dustproof, waterproof, and explosion-proof were also considered during the sensors installation process. The bulldozer vibrates greatly during work. Therefore, the fixing of hardware also considered the problem of shock absorption. The shock absorber was fixed on the bolt to reduce vibration and improved the reliability of the hardware. After each hardware installation was completed, a functional test was carried out to ensure that the hardware functions were intact. The integration test of the subsystems was carried out after installation, including environmental perception, communication, blade leveling, and control systems.

Figure 8 shows the scene information collected by the camera on the top of the modified bulldozer cab. This is the bulldozer modification monitoring system with independent path planning ability designed by us. The cameras are located in different directions to record the environment around the bulldozer. Combined with the position estimation of bulldozer and the preprocessing of sensor, the scene is uploaded to the platform for collision free path planning.

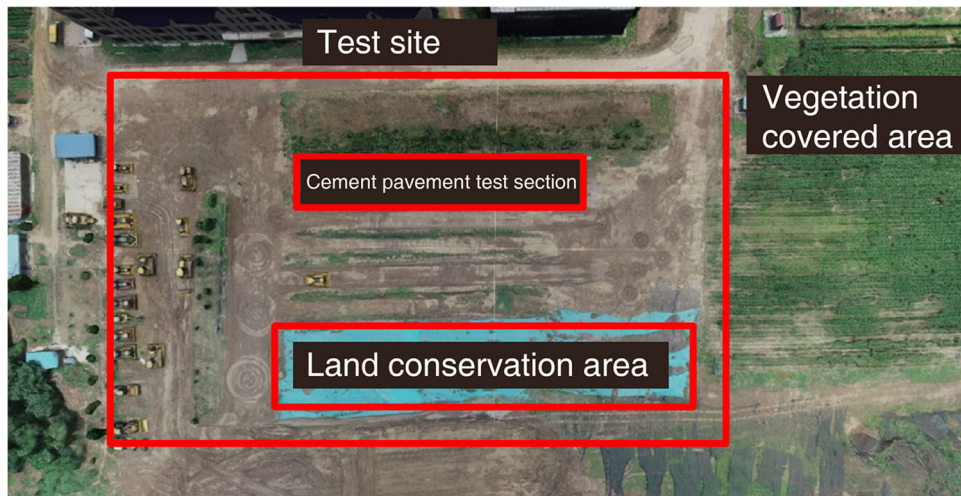


**FIGURE 7** Real scene model map.

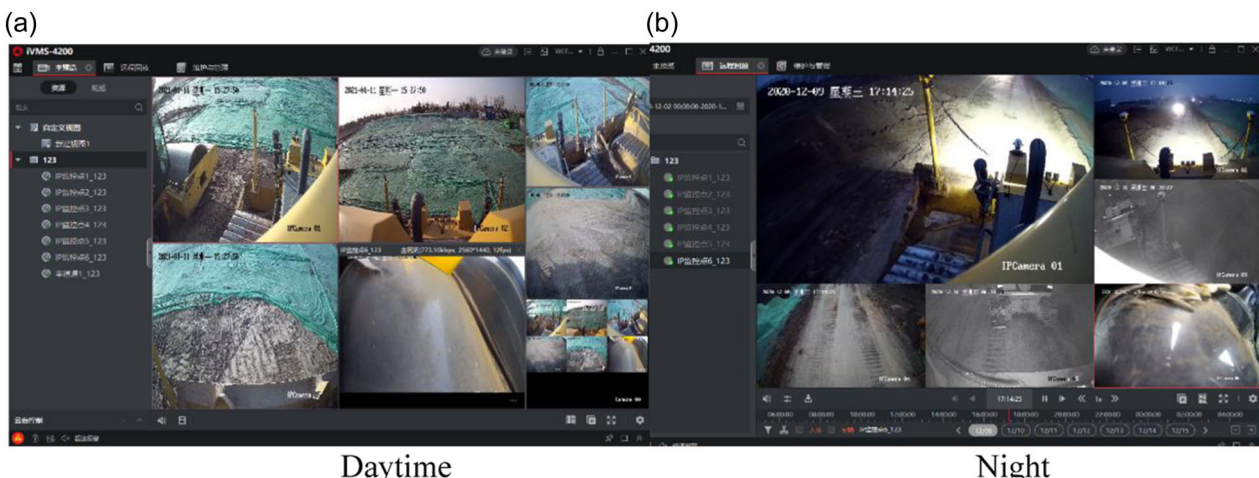


**FIGURE 8** Site information collected by camera.

## 4.3 | Test results

### 4.3.1 | Generation of the occupancy grid map

According to the process in Figure 6, the navigation map in Figure 9 can be generated for path planning. The specific size of the cell is the distance between the path control points determined by the calculated bulldozer



**FIGURE 9** Final occupancy grid map for navigation.

volume and the scope of the construction site. As can be seen from the figure, the working environment is divided into square units with a precise shape. If obstacles, such as mound/soil slope, machinery, or large trees, were found in the 3D model with a height/depth of more than 2 m, they need to be demarcated, because the maximum working height of a bulldozer is 2 m, if the vertical drop of a mound was more than 2 m, the bulldozer would not work, which might cause damage to the mechanical part of the bulldozer and bring unnecessary cost loss. Due to the large scale of the construction site, there are no detailed requirements for the classification of similar grids. Therefore, the “0-1 mapping method” is selected in the occupancy rules. If the proportion of obstacles in a cell is less than one cell, it is still regarded as occupying one cell. This unit is regarded as an obstacle unit and is not allowed to pass. After the division of the construction area, the entrance of the bulldozer into the site should be selected as the starting point of the complete coverage path.

### 4.3.2 | The results of CCPP

As shown in Figure 10, there are four cases from the top view of the site. Basic information is established, which the obstacles are

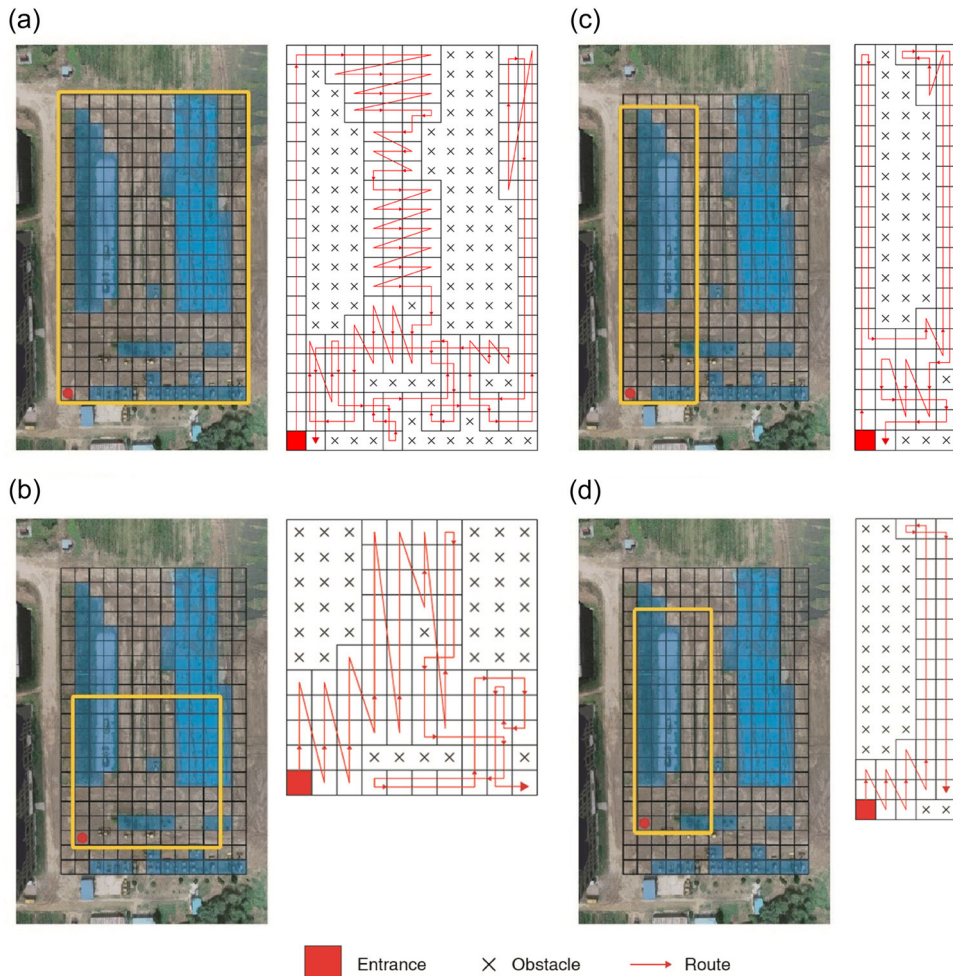


**FIGURE 10** Different case study and results.

presented in blue color, the red cell is the entrance, and the yellow framed area is different test sections, which is also the construction site test area. Case (a) is the path planning of all scanning fields. The entire site is completely covered. Cases (b) and (c) are two different sizes of the sites, but the area of the obstacles in the sites are the same. And the shape of the site in (b) is a square field, and in (c) is a rectangular field. Case (d) is similar to the rectangular site in (c), but the area is smaller than that in (c). The goal is to level the construction area roughly within the yellow framed area. In accordance with the scenarios, we use the CCPP algorithm to obtain formal results of bulldozers in the actual sites. The right images of (a), (b), (c), and (d) are the path planning results, and each result corresponds to a case. The fork is used to identify the area where the obstacle is located, the red cell is the entrance point where the path starts from, and the red line with an arrow is the path and walking direction. Especially, the diagonal line is the real operation rule that our bulldozer moves forward and backward to minimize turning.

#### 4.4 | Application on the autonomous bulldozers

We tested the system on the modified bulldozer. The digital construction platform combines the modeling of UAV with the obstacle map identified by sensors, generates the complete coverage path planning through the proposed BINN hybrid A\* algorithm, and sends it to the vehicle platform. The Tbox was installed on the vehicle in the bulldozer cab, the final display interface and the path planning interface are shown in Figure 11. Site experiment showed that we have achieved path planning on the automatic bulldozer with auxiliary construction equipment. This study only experimented with typical construction scenarios and did not cover all working conditions of bulldozers. Therefore, there are some limitations, including the insufficiently rich experimental data and the insufficiently complex action of bulldozers. The research on the test of unmanned bulldozer is still continuing despite the presence of many difficulties and challenges.

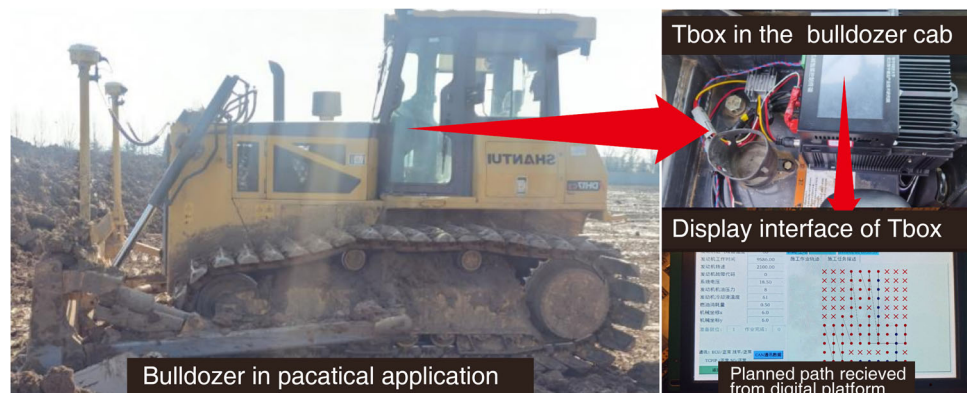


**FIGURE 11** Application of CCPP on the modified bulldozer.

## 5 | CCPP ALGORITHM EVALUATION AND PERFORMANCE FACTOR ANALYSIS

### 5.1 | Evaluation of the CCPP

#### 5.1.1 | Effectiveness of the algorithm

When there is only traditional BINN algorithm added operation rules, the conditions that the local side connection points of the current point have the same neuron activity value, appear easily, which increased the length of the planned path, the repetition rate, and the number of turns. When bulldozer falls into a dead zone, A\* algorithm could help to escape and experiments were conducted as follow to verify the effectiveness of CCPP algorithm.

As indicated in Figure 12, Cases (a), (b), (c), and (d) in Figure 10 were selected to perform comparative experiments. CCPP algorithm, when applied to bulldozers, decreases the path length, number of turns, and repetition rate and is capable of complete coverage. Because Scene (d) is relatively simple, no difference is observed regardless of whether A\* is used or not. Different states of bulldozers trigger different rules that guide the moving direction and next position; this situation addresses the problem of having too many turns and high repetition rate of the path in the original method, as shown in Tables 1, 2, and 3. Moreover, adding A\* algorithm worked well in Scenes (a), (b) and (c). When the A\* algorithm was introduced, the agent could escape from the dead zone by traversing an improved path and can continue to cover the task in the next stage. The simulation experiment with MATLAB shows the effectiveness of the improved method.

#### 5.1.2 | Applicability of the CCPP on site

To verify the applicability and correctness of CCPP algorithm, we let a bulldozer operator perform rough leveling work in Case (d), and collected real-time RTK data on the bulldozer to reflect the real-time construction path of the manned bulldozer, to compare with the autonomous path generated by CCPP method to prove the consistency

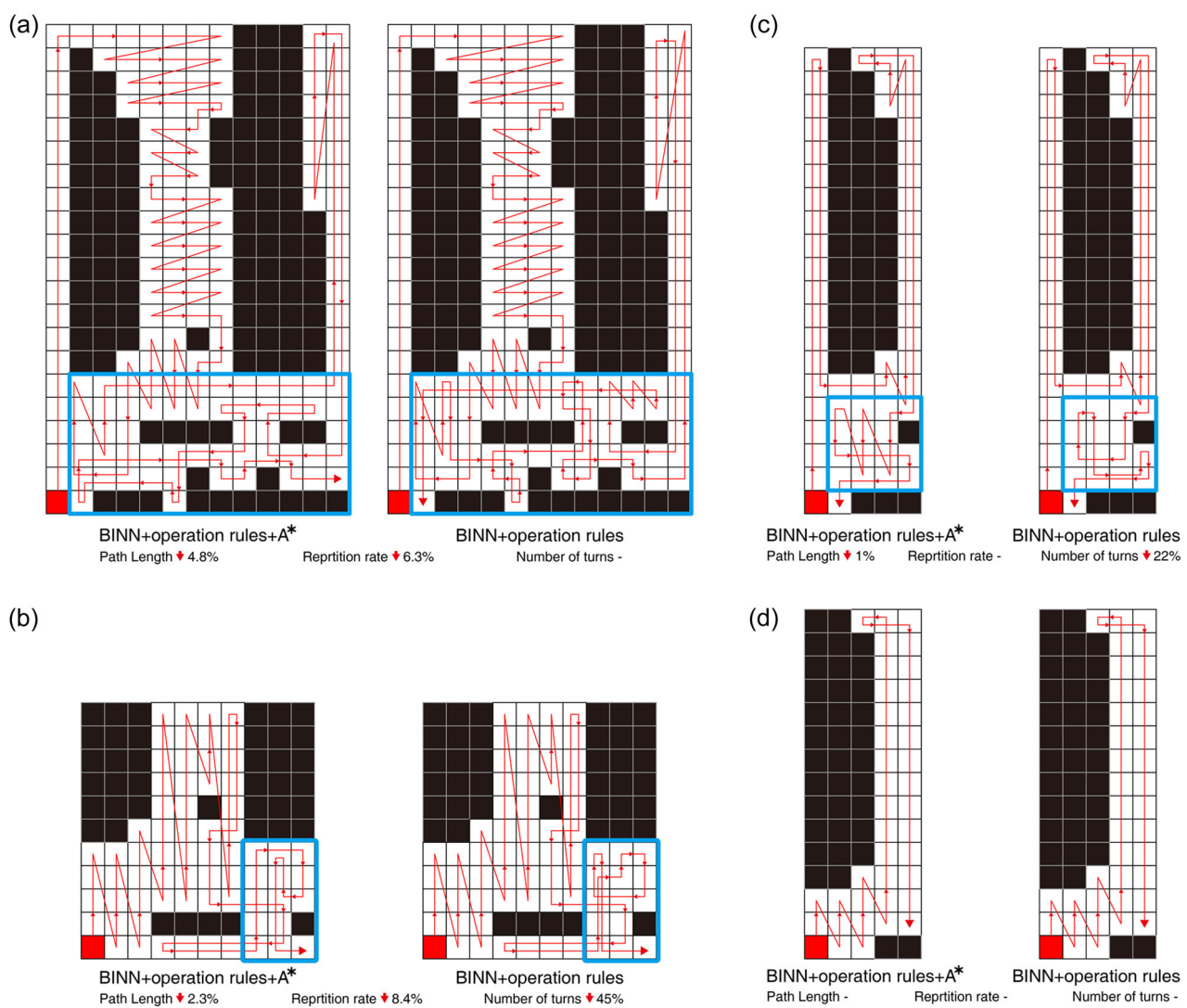


**FIGURE 12** Planned paths under different algorithms.

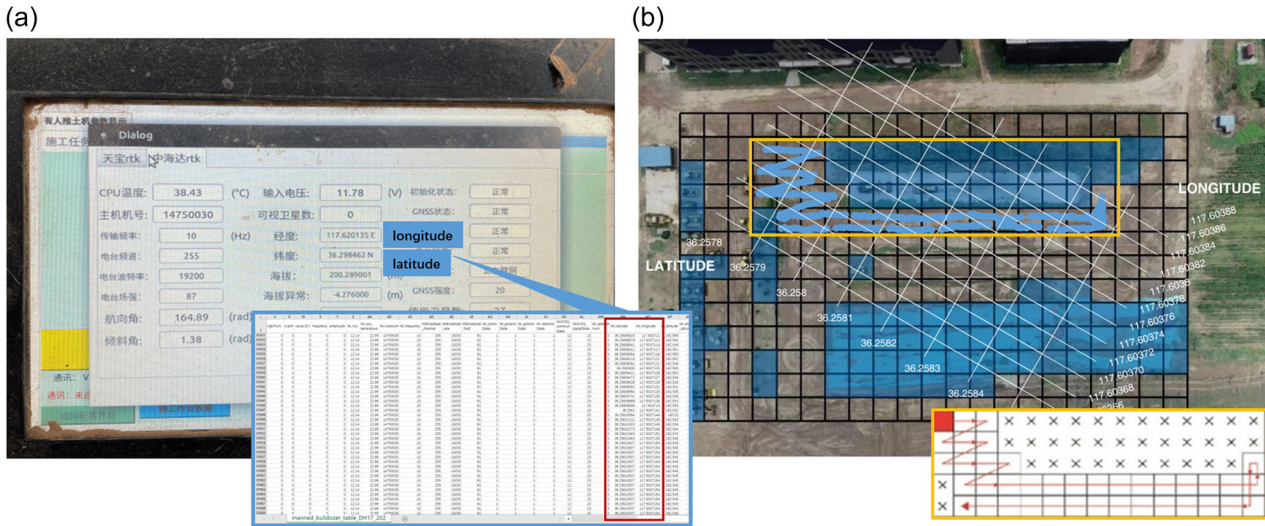
**TABLE 1** Results of Scene (a)

	Path length	Number of turns	Repetition rate (%)	Coverage rate (%)
BINN	257	67	36.97	100
BINN + operation rules	210	38	32.07	100
BINN + operation rules + A*	200	39	25.79	100

**TABLE 2** Results of Scene (b)

	Path length	Number of turns	Repetition rate (%)	Coverage rate (%)
BINN	116	44	40.52	100
BINN + operation rules	88	20	21.59	100
BINN + operation rules + A*	86	11	19.77	100

	Path length	Number of turns	Repetition rate (%)	Coverage rate (%)
BINN	102	20	42.16	100
BINN + operation rules	94	18	37.23	100
BINN + operation rules + A*	93	14	37.63	100

**TABLE 3** Results of Scene (c)**FIGURE 13** Manned bulldozer data collection on site.

with the construction operation rules and habits of a skilled operator on actual construction site. As shown in Figure 13, 13a is the interface of the Tbox on the manned bulldozer, which displayed the real-time position of the bulldozer (RTK latitude and longitude), the location points of the time series were connected to form a path in Figure 13b. It can be seen that in the same scenario, the path generated by our algorithm is in line with the operating of the bulldozer operator. Thus, the suitability of the proposed algorithms effectively reflected the skilled operator's work pattern. If it is used to command an unmanned bulldozer, it can also be well applied to on-site construction.

In the process of improvement, our understanding of bulldozer operation rules and the cooperation of software and hardware ensure the timely realization of each process and assumption. Taking into account the situation of the construction site, the intelligent path planning algorithm can greatly improve construction efficiency.

The automatically planned coverage path can support the efficiency and accuracy of the bulldozer in the limited resources and space. Among all relevant personnel, the bulldozer operator on site is the one who is the most familiar with the requirements and working path of the bulldozer. As an operator with 15-years-experience said (translated in English):

We used to have headaches for repetitive actions when rough leveling. Now, it would be great if there were

autonomous bulldozers to help replace this stage of work. The results of the path planning so far are quite accurate. It is quite in line with the actual on-site construction situation. If it can become dynamic in the future, and then add construction techniques for other working conditions, perhaps the application prospects will be broader, I think.

The method can reduce the workload of certain workers at this stage. There are still situations where construction workers supervise and direct the operation of bulldozers. The UAV-based modeling in advance to generate a map and algorithms to automatically generate a path to command the unmanned bulldozer, can also greatly reduce the input of on-site personnel. As an on-site supervisor said (translated in English):

I feel that the path can be automatically planned is very practical, these paths are suitable for on-site, whether it is used to guide the operation of the bulldozer operator or used for the unmanned bulldozer, it greatly reduces our workload. I checked these planned paths, generally speaking, they were not much different from our usual bulldozer rough leveling work habits, and there were even more optimized places.

## 5.2 | Different factors analysis

We configure the same environmental condition with (c) in the program made in MATLAB, create a total of  $5 \times 17$  grids, and set the starting point, as shown in Figure 14. In the figure, the black part indicates the area that cannot be walked on, according to rules in Section 4.3.1, and the red part refers to the path that passed. The algorithm can ensure full coverage of the path; the coverage rate is 100%, and all obstacles are avoided. Hence, is effective when applied in the construction field. The site is 75 m long (effective transportation distance of the bulldozer), 25 m wide (width of a two-way four-car road base), and 5 m  $\times$  5 m per unit size (determined by bulldozer volume, calculated construction range, and bulldozer automatic positioning unit characteristics) (Table 4).

In Table 5, X, Y, and Z are variable factors during the test. X represents the entrance position, which has three conditions: bulldozer entering the site beginning to work from the corner point, the trisection point and the midpoint of the entrance edge. Y represents the position of the obstacles. As shown in the illustration, obstacles could lie in the corners, the sides and the middle of the site. And there are four corners, four sides for a rectangular site. So, we use two numbers behind Y to distinguish between these situations, such as Y1-(Y11, Y12, Y13, Y14), Y2-(Y21, Y22, Y23, Y24). Z represents the shape of the obstacles which is also divided into three kinds.

A total of 66 cases are considered, except for the overlap of repetition, obstacles, and entrances. Some cases are selectively shown in Figure 14. These experiments can be divided into the

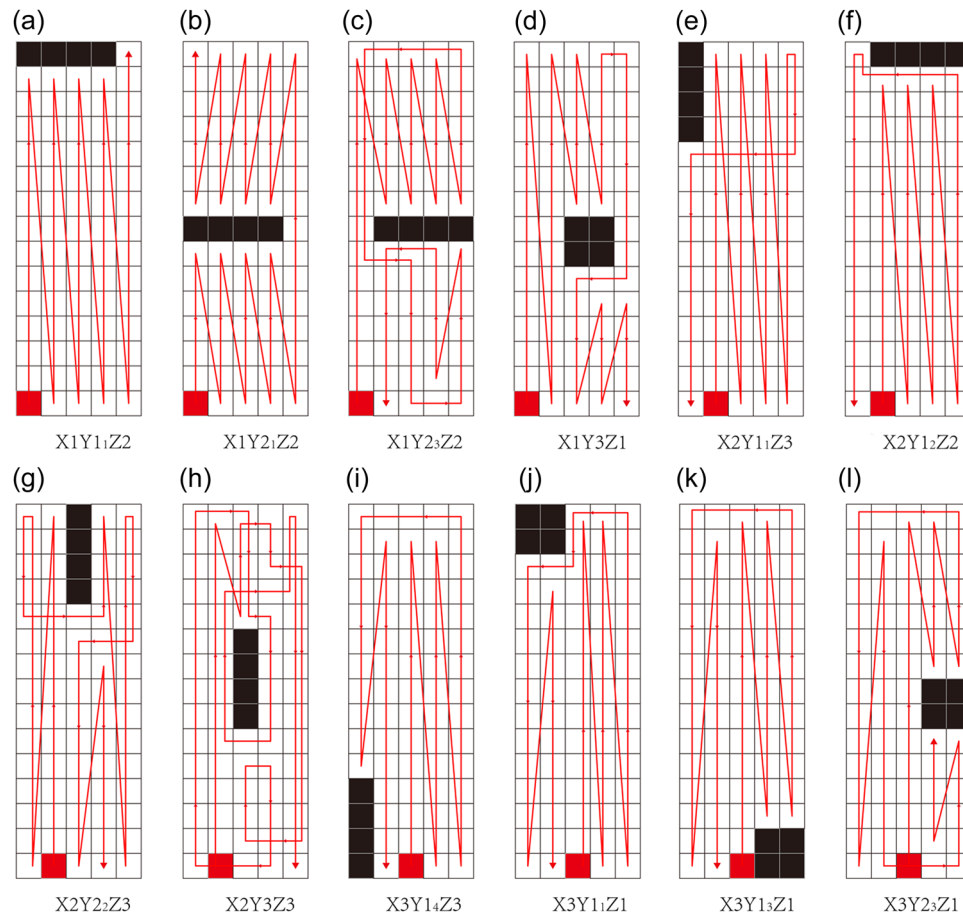


**FIGURE 14** Variable cases.

**TABLE 4** Results of Scene (d)

	Path length	Number of turns	Repetition rate (%)	Coverage rate (%)
BINN	44	13	11.36	100
BINN + operation rules	40	3	2.50	100
BINN + operation rules + A*	40	3	2.50	100

Factors	Types	Illustration
X	X1: corner point	
	X2: trisection point	
	X3: edge midpoint	
Y	Y1: four corners	
	Y2: four sides	
	Y3: middle	
Z	Z1: square	
	Z2: rectangle(horizontal to the entrance edge)	
	Z3: rectangle (vertical to the entrance edge)	

TABLE 5 Variable factors

following types: (1) Fix the area and perimeter of the site, the size and shape of the obstacles, and the location of the entrance. Change the location of the obstacles. (2) Fix the area and perimeter of the site and the size, shape, and position of the obstacles. Change the entrance position. (3) Fix the area of the site, the size and location of the obstacles, and the location of the entrance. Change the shape of the obstacles.

The 66 cases' results are shown in Figure 15. In each subgraph, different colors represent different cases, and the three axes represent three evaluation indexes: path length, turning times, and path repetition rate. From (a) to (c) are the distribution classification data of variable X, and (a) is the whole effective cases of all combinations of the other two factors Y, Z in cases of X1 (the entrance is located at the corner of the site), which are a total of 23 groups. (b) and (c) are the whole effective cases in cases of X2 and X3 (the entrance is located at the trisection and mid-edge of the site), which are a total of 22 groups and 21 groups. Similarly, from (d) to (f) are the results of Y variables, the rest (g), (h), and (i) are the results of factor Z. The shape and area of the triangle color coil can intuitively reflect the comprehensive size of the three indicators. The larger the scope of the color coil, the larger the three indicators are. In the construction site, our goal is to reduce the complete coverage path length and the number of turns, as well as the repetition rate, so the smaller the area of the color coil, the more favorable the site layout is for the earthwork. The data from the corner point (such as X1) and the middle point of the side (such as X3) for the entrance are better, which can be seen from the smaller area of the triangle color coil, indicating that it is conducive to the complete coverage path planning; when the obstacle is located at the corner (such as Y1), we could find that the overall area of the color coils are less than that in Y2 and Y3, which can reduce the repetition rate and the number of turns. The analysis of path length, turning times, repetition rate, and coverage rate reveals the applicability of the complete coverage path planning algorithm, by which suggestions are put forward for the

selection of actual construction sites, the existence of obstacles, and the selection of mechanical channels. However, as the number of samples in this experiment is not large enough, it may not be able to expand to a wider range.

### 5.2.1 | External factors analysis

Table 6 shows the significance and correlation between each site factor and path length, turning times, and path repetition rate. Testing of the subjectivity effect shows that the entry position of the bulldozer (X factor) and the position of obstacles (Y factor) exert a considerable influence on the CCPP algorithm. The shape of obstacles is not the main factor. Therefore, in future project sites, the selection of the bulldozer construction path must consider the location of bulldozer approach and the location of obstacles in the sites. The algorithm achieves good full coverage, as evidenced by the 100% coverage. Factor X, that is, bulldozer entrance position, has the highest correlation with each evaluation index ( $p = 0.000$ ). Factor Y (obstacle position) also has a significant correlation ( $p < 0.05$ ) with path length, turn times, and path repetition rate. Meanwhile, the correlation between obstacle shape and the evaluation indexes is not significant ( $p > 0.05$ ), and the  $p$  value is large, which may lead to an unreasonable setting. Therefore, factor Z is not considered in the subsequent discussion and research. As shown in Figures 15 and 16, the statistical values of all the experimental results are related to factors X and Y.

In Figure 16a, regardless of where the obstacle is, the average path length, turning times, and path repetition are the smallest when the entrance position is at the corner (factor X1), which shows the entrance at the corner has the best impact on construction path. We also observe differences in factor Y. When the obstacles are in the corner (factors Y11, Y12, and Y13), these evaluation indicators also perform better than they do in the other situations in Figure 16b. The

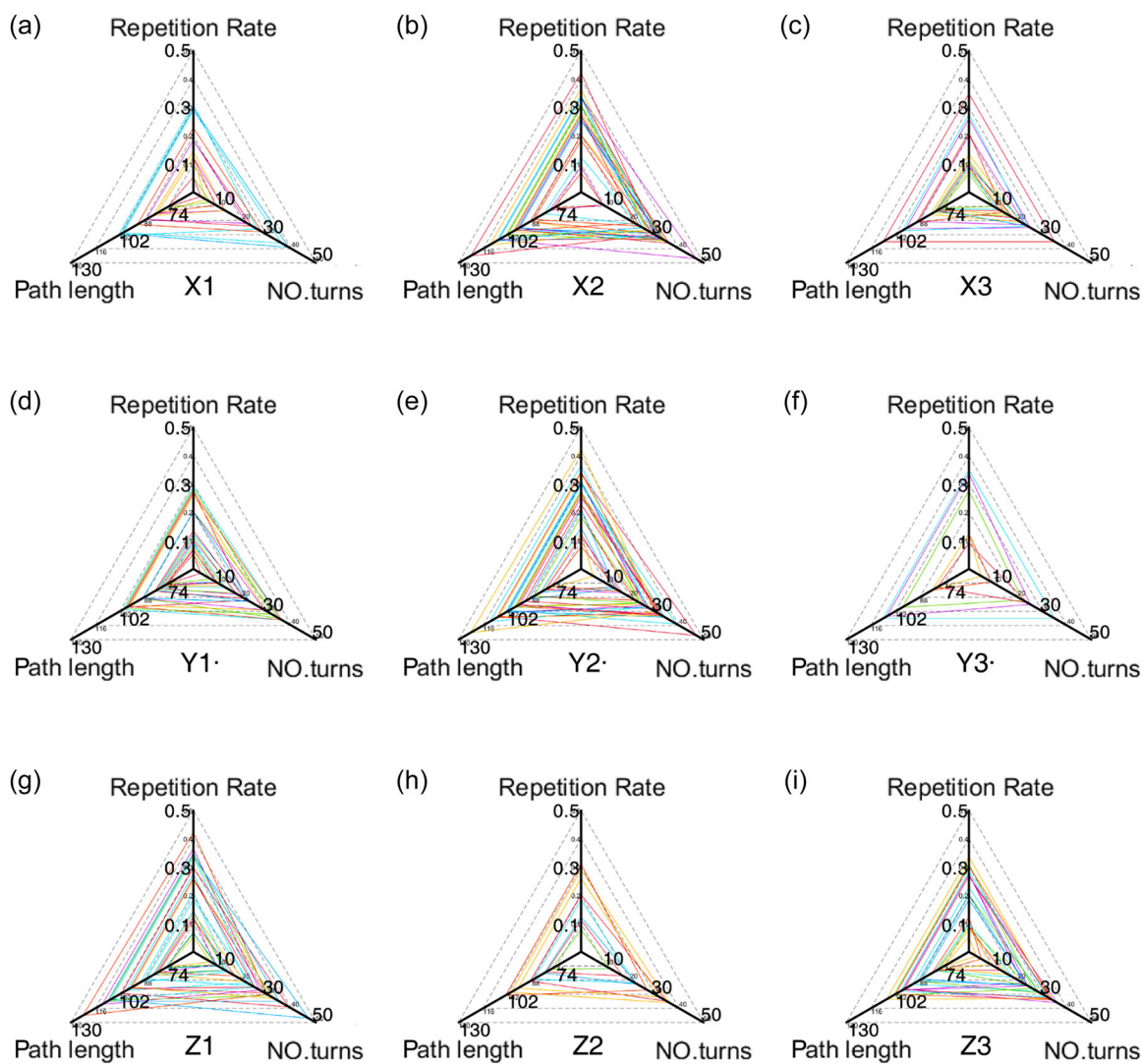


**FIGURE 15** Results of the 66 cases. (a–c) The distribution classification data of variable X, different colors represent different cases; (d–f) The distribution classification data of variable Y; (g–i) The distribution classification data of variable Z.

**TABLE 6** The relevance results of the factors.

	Dependent variable	p value
X	Path length	0
	Number of turns	0
	Repetition rate	0
Y	Path length	0.002
	Number of turns	0.023
	Repetition rate	0
Z	Path length	0.295
	Number of turns	0.989
	Repetition rate	0.361

bulldozer can walk randomly according to the neuron activity value only when the position of the obstacle makes the bulldozer initialize its own forward and backward walking rules as early as possible after starting from the entrance. As a result, the path is shortened, the

number of turns is reduced, and the repetition rate decreases. For example, if the obstacle on site is regarded as Y13Z3, then we could choose the entrance to start earthwork at X1, which would achieve better results, reduce the length of the construction path, turns and repetition rate, helping improve construction efficiency, as shown in Figure 17. In future research, we can add the step of dividing the subject region by using the algorithm, which moves forward and backward according to the rules rather than searching the path immediately according to the active value without the trigger rules.

### 5.2.2 | Internal factors analysis

According to the previous analysis of algorithm parameters, this section carries out the best combination experiment of  $A$  and  $u$ . According to Meng's research (1998), the value range of  $A$  and  $u$  was  $A = 10, A = 20, A = 50, A = 100, u = 0.005, u = 0.01, u = 0.025, u = 0.05, u = 0.1, u = 0.25, u = 0.5, u = 0.75$  and  $u = 1$ . Experiment was carried out three times for each group of parameters to avoid

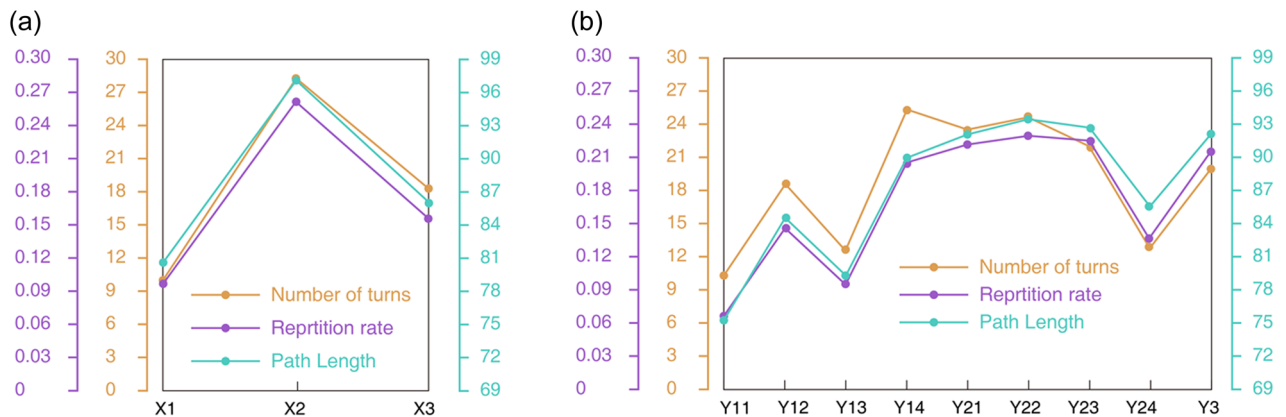


**FIGURE 16** Influence of factor X and factor Y.



**FIGURE 17** Entrance choice for real scene.

accident. Figure 9 Scene (c) was selected to study the optimal combination of parameters  $A$  and  $u$  in the improved algorithm, which could minimize the number of turns and the path repetition rate. The experimental results are shown in Table 7.

According to the experimental results in Table 7, when  $A = 20$ ,  $B = 1$ ,  $d = 1$ ,  $E = 100$ ,  $u = 0.01$ , and  $A = 100$ ,  $B = 1$ ,  $d = 1$ ,  $E = 100$ ,  $u = 0.01$ , the path planning results can reach the optimal. The parameter combination of the above two groups of algorithms is the optimal parameter combination of the method.

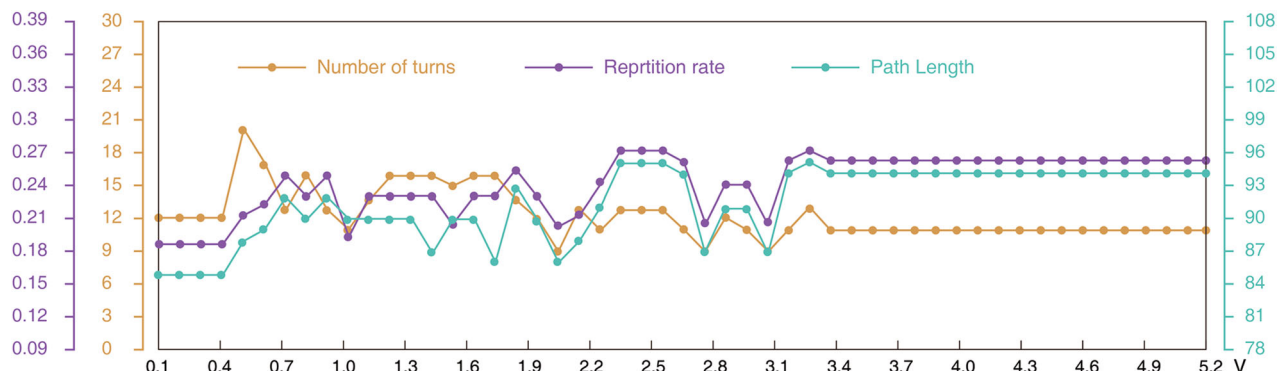
At the same time, we adopted ode45 in MATLAB as the neuron activity value solver, which was the preferred method to solve the numerical solution problem. It could be seen that the setting of sampling time  $tspan$  also affected the result of overall path planning. As shown in Figure 17, when  $A = 100$ ,  $B = 1$ ,  $d = 1$ ,  $E = 100$ ,  $u = 0.01$ , the results of path planning in different cases with  $tspan$  ranging from 0.2 to 10 are tested. We changed searching speed  $V$ , that is, we

changed the sampling time (sampling time  $tspan = 1/V$ ), to analyze the impact on the algorithm. Forty-five groups of experiments were conducted from  $V = 0.1$  to 4.5. The results are shown in Figure 18.

We find that this sampling time affects the algorithm. Sampling time length sometimes affects the acquisition and iteration of information. Hence, as shown in Figure 17, with the increase in search speed, path length, and repetition rate exhibit increased oscillation, and the number of turns shows decreased oscillation. However, after  $V = 3.3$ , the three indicators stabilize. Several global constant parameters should also be considered when algorithm problems occur in the iteration of path planning. If these parameters are randomly selected, different situations will occur easily, and even the simulation results will be affected to a certain extent. After establishing this rule, we can verify the influence of parameter setting through subsequent experiments, identify a stable range, and perform simulations.

**TABLE 7** Path planning results with different algorithm parameters.

A	u	Path length	No. turn	Repetition rate (%)	Coverage rate (%)	A	u	Path length	No. turn	Repetition rate (%)	Coverage rate (%)
10	1	73	8	17.81	100	50	1	72	6	16.67	100
	0.75	73	8	17.81	100		0.75	72	6	16.67	100
	0.5	74	6	18.92	100		0.5	72	6	16.67	100
	0.25	72	5	16.67	100		0.25	64	8	6.25	100
	0.1	64	8	6.25	100		0.1	64	8	6.25	100
	0.05	63	7	4.76	100		0.05	64	8	6.25	100
	0.025	65	6	7.69	100		0.025	64	8	6.25	100
	0.01	65	6	7.69	100		0.01	64	8	6.25	100
	0.005	64	8	6.25	100		0.005	64	8	6.25	100
20	1	72	6	16.67	100	100	1	73	8	17.81	100
	0.75	72	6	16.67	100		0.75	72	6	16.67	100
	0.5	74	6	18.92	100		0.5	64	8	6.25	100
	0.25	74	6	18.92	100		0.25	64	8	6.25	100
	0.1	76	10	21.05	100		0.1	64	8	6.25	100
	0.05	65	5	7.69	100		0.05	64	8	6.25	100
	0.025	64	8	6.25	100		0.025	64	8	6.25	100
	0.01	62	4	3.23	100		0.01	62	4	3.23	100
	0.005	64	8	6.25	100		0.005	64	8	6.25	100

**FIGURE 18** Influence of factor tspan.

## 6 | CONCLUSION

In this paper, a CCPP method based on BINN hybrid A\* algorithm is proposed for the rough leveling process, and various factors affecting the method are analyzed. At the same time, a modified bulldozer with monitoring system and autonomous path planning ability is designed, and an integrated framework of automatic bulldozer complete coverage path planning is proposed to implement the application of the algorithm. According to the simulation experiment, reasonable suggestions are put forward for the selection of entrance location, site layout and planning, site obstacles, and so on.

When the BINN algorithm is used to add bulldozer operation rules for complete coverage path planning, the entrance position exerts the greatest impact on the path. Placing the entrance position in a corner can improve the performance of the indicators of the coverage path. The position of obstacles also influences the bulldozer path. When the obstacles in the site cannot be moved, an appropriate entrance position should be selected so that the bulldozer will have space for the complete and efficient execution of construction rules and can move backward from the syncline. Otherwise, unnecessary turning and repetition will increase.

Our study has limitations, which can be improved in the future. First, when the algorithm encounters scenes that disrupt forward and

backward rules, it divides the area first and the blocks afterward to follow the forward and backward rules rather than search the path immediately following the active value. Second, in future research, additional restrictions, such as regulation and exit location and establishment of the most effective operating distance, can be set to study other factors for bulldozing. The effects of the complete coverage path of the vehicle in the site should also be examined. Third, future research can add the information of elevation change as a construction working condition into the algorithm setting. This consideration can guide bulldozers as they push back and forth several times in a certain place during construction. And additional experiments will be conducted in future work to test the reliability of the earthwork monitoring system for the unmanned bulldozer. The research on the test of unmanned bulldozer is still continuing despite the presence of many difficulties and challenges.

## NOMENCLATURES

AUV	autonomous unmanned vehicle
BINN	bioinspired neural network
CCPP	complete coverage path planning
GNSS	global satellite navigation system
IMU	inertial measuring unit
LIDAR	light detection and ranging
RTK	real-time kinematic
UAV	unmanned Aerial Vehicle

## ACKNOWLEDGMENTS

This study is supported in part by the National Natural Science Foundation of China (71732001 and 71821001). This study is also supported by Major Science and Technology Project of Hubei (No. 2020ACA006). This study is also supported by Weichai Power Co., Ltd. and Shantui Construction Machinery Co., Ltd. The authors thank Shantui Construction Machinery Co., Ltd. Special thanks to the reviewers and the editors for their valuable comments and thorough editing efforts. Their contributions have significantly improved the work.

## DATA AVAILABILITY STATEMENT

Research data are not shared.

## REFERENCES

- AlBahnassi, H. & Hammad, A. (2012) Near real-time motion planning and simulation of cranes in construction: framework and system architecture. *Journal of Computing in Civil Engineering*, 26(1), 54–63. Available from: [https://doi.org/10.1061/\(ASCE\)CP.1943-5487.0000123](https://doi.org/10.1061/(ASCE)CP.1943-5487.0000123)
- Ali Roshanianfard, A., Noguchi, N., Okamoto, H. & Ishii, K. (2020) A review of autonomous agricultural vehicles (The experience of Hokkaido University). *Journal of Terramechanics*, 91, 155–183. Available from: <https://doi.org/10.1016/j.jterra.2020.06.006>
- Alshaer, B.J., Darabseh, T.T. & Alhanouti, M.A. (2013) Path planning, modeling and simulation of an autonomous articulated heavy construction machine performing a loading cycle. *Applied Mathematical Modelling*, 37(7), 5315–5325. Available from: <https://doi.org/10.1016/j.apm.2012.10.042>
- An, J., Wu, M., She, J. & Terano, T. (2018) Re-optimization strategy for truck crane lift-path planning. *Automatic Construction*, 90, 146–155. Available from: <https://doi.org/10.1016/j.autcon.2018.02.029>
- Barbosa, F., Woetzel, J., Mischke, J., Ribeirinho, M.J., Sridhar, M. & Parsons, M. et al. (2017) Reinventing construction: a route to higher productivity. Available at: McKinsey Global Institute. <https://www.mckinsey.com/industries/capital-projects-and-infrastructure/our-insights/reinventing-construction-through-a-productivity-revolution>
- Bonchis, A., Hillier, N., Ryde, J., Duff, E. & Pradalier, C. (2016) Experiments in autonomous earth moving. 18th IFAC World Congress (IFAC 2011), Milano, Italy, August 28–September 2, 2011, Elsevier Vol 44: 11593. Available from: <https://doi.org/10.3182/20110828-6-IT-1002.00536>
- Cai, P., Cai, Y., Chandrasekaran, I. & Zheng, J. (2016) Parallel genetic algorithm based automatic path planning for crane lifting in complex environments. *Automatic Construction*, 62, 133–147. Available from: <https://doi.org/10.1016/j.autcon.2015.09.007>
- Chang, Y.C., Hung, W.H. & Kang, S.C. (2012) A fast path planning method for single and dual crane erections. *Automatic Construction*, 22, 468–480. Available from: <https://doi.org/10.1016/j.autcon.2011.11.006>
- Chen, Q., García de Soto, B. & Adey, B.T. (2018) Construction automation: research areas, industry concerns and suggestions for advancement. *Automatic Construction*, 94, 22–38. Available from: <https://doi.org/10.1016/j.autcon.2018.05.028>
- Dakulović, M., Horvatić, S. & Petrović, I. (2011) Complete coverage d\* algorithm for path planning of a floor-cleaning mobile robot. *IFAC Proceedings Volumes*, 44(1), 5950–5955. Available from: <https://doi.org/10.3182/20110828-6-IT-1002.03400>
- Dogru, S. & Marques, L. (2015) Marques energy efficient coverage path planning for autonomous mobile robots on 3D terrain. In: *2015 IEEE International Conference on Autonomous Robot Systems and Competitions*. Available from: <https://doi.org/10.1109/ICARSC.2015.23>
- Fang, Y., Cho, Y.K. & Durso, F. (2018) Assessment of operator's situation awareness for smart operation of mobile cranes. *Automatic Construction*, 85, 65–75. Available from: <https://doi.org/10.1016/j.autcon.2017.10.007>
- Guastella, D., Cantelli, L., Giannello, G., Melita, C.D., Spatino, G. & Muscato, G. (2019) Complete coverage path planning for aerial vehicle flocks deployed in outdoor environments. *Computers & Electrical Engineering*, 75, 189–201. Available from: <https://doi.org/10.1016/j.compeleceng.2019.02.024>
- Han, S., Lei, Z., Bouferguene, A., Al-Hussein, M. & Hermann, U. (2016) 3D visualization-based motion planning of mobile crane operations in heavy industrial projects. *Journal of Computing in Civil Engineering*, 30(1), 04014127. Available from: [https://doi.org/10.1061/\(ASCE\)CP.1943-5487.0000467](https://doi.org/10.1061/(ASCE)CP.1943-5487.0000467)
- Hayashi, K., Shimada, K., Ishibashi, E., Okamoto, K. & Yonezawa, Y. (2013) Development of D 61EXi/PXi-23, Bulldozer with automatic control system of work equipment. *Komatsu Technical Report*, No. 166.
- Hirayama, M., Guivant, J., Katupitiya, J. & Whitty, M. (2019) Path planning for autonomous bulldozers. *Mechatronics*, 58, 20–38. Available from: <https://doi.org/10.1016/j.mechatronics.2019.01.001>
- Hirayama, M., Whitty, M., Katupitiya, J. & Guivant, J. (2018) An optimized approach for automatic material distribution operations of bulldozers. *International Journal of Advanced Robotic Systems*, 15(2), 172988141876471. Available from: <https://doi.org/10.1177/1729881418764716>
- Hung, W.H., Liu, C.W., Liang, C.J. & Kang, S.C. (2016) Strategies to accelerate the computation of erection paths for construction cranes. *Automatic Construction*, 62, 1–13. Available from: <https://doi.org/10.1016/j.autcon.2015.10.008>

- Jonasson, S., Dunston, P.S., Ahmed, K. & Hamilton, J. (2002) Factors in productivity and unit cost for advanced machine guidance. *Journal of Construction Engineering and Management*, 128(5), 367–374. Available at [https://doi.org/10.1061/\(ASCE\)0733-9364\(2002\)128:5\(367\)](https://doi.org/10.1061/(ASCE)0733-9364(2002)128:5(367))
- Karapetyan, N., Benson, K., McKinney, C., Taslakian, P. & Rekleitis, I. (2017) Efficient Multi-Robot Coverage of a Known Environment. In: 2017 IEEE/RSJ International Conference on Intelligent Robots and Systems (IROS). <https://doi.org/10.1109/IROS.2017.8206000>
- Kim, J., Lee, D. & Seo, J. (2020) Task planning strategy and path similarity analysis for an autonomous excavator. *Automatic Construction*, 112, 103–108. Available from: <https://doi.org/10.1016/j.autcon.2020.103108>
- Kim, S., Lee, Y.S., Sun, D.I., Lee, S.K., Yu, B.H. & Jang, S.H. et al. (2019) Development of bulldozer sensor system for estimating the position of blade cutting edge. *Automatic Construction*, 106, 102890. Available from: <https://doi.org/10.1016/j.autcon.2019.102890>
- Kim, S.K. & Russell, J.S. (2013) Framework for an intelligent earthwork system. *Automatic Construction*, 12(1), 15–27. Available from: [https://doi.org/10.1016/s0926-5805\(02\)00033-x](https://doi.org/10.1016/s0926-5805(02)00033-x)
- Kim, S.K. & Seo, J. (2012) Intelligent navigation strategies for an automated earthwork system. *Automatic Construction*, 21, 132–147. Available from: <https://doi.org/10.1016/j.autcon.2011.05.021>
- Kun, Z. (2020) Method and bench-marking framework for coverage path planning in arable farming. *Biosystems Engineering*, 198, 248–265. Available from: <https://doi.org/10.1016/j.biosystemseng.2020.08.007>
- Lakshmanan, A., Mohan, R.E., Ramalingam, B., Le, A.V., Veerajagadeeshwar, P., Tiwari, K. & Ilyas, M. (2020) Complete coverage path planning using reinforcement learning for Tetromino based cleaning and maintenance robot. *Automatic Construction*, 112, 103078. Available from: <https://doi.org/10.1016/j.autcon.2020.103078>
- Lee, C.S., Bae, J. & Hong, D. (2013) Contour control for leveling work with robotic excavator. *International Journal of Precision Engineering and Manufacturing*, 14, 2055–2060. Available from: <https://doi.org/10.1007/s12541-013-0278-5>
- Leica Geosystems. (2019) Machine control systems. <https://leica-geosystems.com/en-us/products/machine-control-systems> [Accessed 18th May 2019].
- Lin, J.J.C., Hung, W.H. & Kang, S.C. (2014) Motion planning and coordination for mobile construction machinery. *Journal of Computing in Civil Engineering*, 29(6), 04014082. Available from: [https://doi.org/10.1061/\(ASCE\)CP.1943-5487.0000408](https://doi.org/10.1061/(ASCE)CP.1943-5487.0000408)
- Lin, Y., Wu, D., Wang, X., Wang, X. & Gao, S. (2014) Lift path planning for a nonholonomic crawler crane. *Automatic Construction*, 44, 12–24. Available from: <https://doi.org/10.1016/j.autcon.2014.03.007>
- Liu, D., Wu, Y., Li, S. & Suna, Y. (2016) A real-time monitoring system for lift-thickness control in highway construction. *Automatic Construction*, 63, 27–36. Available from: <https://doi.org/10.1016/j.autcon.2015.12.004>
- Liu, J., Yang, J., Liu, H., Tian, X. & Gao, M. (2017) An improved ant colony algorithm for robot path planning. *Soft Computing*, 21(19), 5829–5839. Available from: <https://doi.org/10.1007/s00500-016-2161-7>
- Liu, J., Yao, W. & Zhang, W. (2019) Research on complete coverage path planning algorithm of mobile robots. *Industrial Control Computer*, 32(12), 52–54.
- Luo, C., Yang, S.X., Li, X. & Meng, M. (2016) Neural-dynamics-driven complete area coverage navigation through cooperation of multiple mobile robots. *IEEE Transactions on Industrial Electronics*, 750–760. Available from: <https://doi.org/10.1109/TIE.2016.2609838>
- Luo, C.M. & Yang, S.X. (2002) A solution to vicinity problem of obstacles in complete coverage path planning. In: *Proceedings 2002 IEEE International Conference on Robotics and Automation* (Cat. No. 02CH37292). Available from: <https://doi.org/10.1109/robot.2002.1013426>
- Meng, M. & Yang, X. (1998) A neural network approach to real-time trajectory generation[mobile robots]. In: *Proceedings of 1998 IEEE International Conference on Robotics and Automation*, pp. 1725–1730. Available from: <https://doi.org/10.1109/ROBOT.1998.677414>
- Minamoto, M., Kawashima, K. & Kanno, T. (2016) Effect of force feedback on a bulldozer-type robot. In: *Proceedings of IEEE International Conference on Mechatronics and Automation*. Available from: <https://doi.org/10.1109/ICMA.2016.7558908>
- Muthugala, M.A.V.J., Samarakoon, S.M.B.P. & Elara, M.R. (2022) Toward energy-efficient online complete coverage path planning of a ship hull maintenance robot based on gladius bio-inspired neural network. *Expert Systems with Applications*, 187, 115940. Available from: <https://doi.org/10.1016/j.eswa.2021.115940>
- Navon, R., Goldschmidt, E. & Shpatnisky, Y. (2004) A concept proving prototype of automated earthmoving control. *Automatic Construction*, 13, 225–239. Available from: <https://doi.org/10.1016/j.autcon.2003.08.002>
- Ni, J., Wu, L., Shi, P. & Yang, S.X. (2017) A dynamic bioinspired neural network based real-time path planning method for autonomous underwater vehicles. *Computational Intelligence and Neuroscience*, 2017, 1–16. Available from: <https://doi.org/10.1155/2017/9269742>
- Nilsson, R.S. & Zhou, K. (2020) Method and bench-marking framework for coverage path planning in arable farming. *Biosystems Engineering*, 198, 248–265. <https://doi.org/10.1016/j.biosystemseng.2020.08.007>
- Sandamurthy, K. & Ramanujam, K. (2019) A hybrid weed optimized coverage path planning technique for autonomous harvesting in cashew orchards. *Information Processing in Agriculture*, 7(1). Available from: <https://doi.org/10.1016/j.inpa.2019.04.002>
- Sivakumar, P., Varghese, K. & Babu, N.R. (2013) Automated path planning of cooperative crane lifts using heuristic search. *Journal of Computing in Civil Engineering*, 17(3), 197–207. Available from: [https://doi.org/10.1061/\(ASCE\)0887-3801\(2003\)17:3\(197\)](https://doi.org/10.1061/(ASCE)0887-3801(2003)17:3(197))
- Sturm, A. & Vos, W. (2008) New technologies for telematics and machine control. In: *Proceedings of 1st International Conference on Machine Control and Guidance*, Zurich, Switzerland.
- Sun, D.I., Kim, S.H., Lee, Y.S., Lee, S.K. & Han, C.S. (2017) Pose and position estimation of dozer blade in 3-dimensional by integration of IMU with Two RTK GPSs. In: 34th International Symposium on Automation and Robotics in Construction. Available from: <https://doi.org/10.22260/ISARC2017/0137>
- Taghavifar, H., Rakheja, S. & Reina, G. (2021) A novel optimal path-planning and following algorithm for wheeled robots on deformable terrains. *Journal of Terramechanics*, 96, 147–157. Available from: <https://doi.org/10.1016/j.jterra.2020.12.001>
- Trimble. (2019) Machine control. Available at: <https://construction.trimble.com/products-and-solutions/machine-control> [Accessed 18th May 2019].
- Wang, X., Wang, W., Yin, X., Xiang, C. & Zhang, Y. (2018) A new grid map construction method for autonomous vehicles. *IFAC-PapersOnLine*, 51, 377–382. Available from: <https://doi.org/10.1016/j.ifacol.2018.10.077>
- Wang, Z. & Bo, Z. (2014) Coverage path planning for mobile robot based on genetic algorithm. In: *2014 IEEE Workshop on Electronics, Computer and Applications (IWECA)*. IEEE. Available from: <https://doi.org/10.1109/iweca.2014.6845726>
- Yang, S. & Luo, C. (2004) A neural network approach to complete coverage path planning. *IEEE Transactions on Systems, Man, and Cybernetics. Part B, Cybernetics*, 34, 718–725. Available from: <https://doi.org/10.1109/tsmc.2003.811769>

- Zhu, D., Tian, C., Sun, B. & Luo, C. (2019) Complete coverage path planning of autonomous underwater vehicle based on GBNN algorithm. *Journal of Intelligent & Robotic Systems*, 94, 237–249. Available from: <https://doi.org/10.1007/s10846-018-0787-7>
- Zhu, D., Xiang, C. & Sun, B. (2018) Biologically inspired self-organizing map applied to task assignment and path planning of an auv system. *IEEE Transactions on Cognitive and Developmental Systems*, 10(99), 304–313. Available from: <https://doi.org/10.1109/TCDS.2017.2727678>

**How to cite this article:** Li, R., Zhou, C., Dou, Q. & Hu, B. (2022) Complete coverage path planning and performance factor analysis for autonomous bulldozer. *Journal of Field Robotics*, 39, 1012–1032.  
<https://doi.org/10.1002/rob.22085>